22

ИНСТИТУТ ЯДЕРНОЙ ФИЗИКИ СО АН СССР

Yu.I. Belchenko

SURFACE NEGATIVE ION PRODUCTION IN ION SOURCES

PREPRINT 91-27

НОВОСИБИРСК

Surfcace Negative Ion Production in Ion Sources

Yu. I. Belchenko

Institute of Nuclear Physics,

630090, Novosibirsk, USSR

ABSTRACT

Experimental and simulated data on surface NI formation are reviewed. Efficiencies of backscattering and ion induced desorption leading to NI production are discussed. Effects of NI secondary emission enhancement due to plasma "activation" of surfaces or due to simultaneous bombardment of electrodes with various particles ("synergetics") are interpreted. NI production efficiency for cathode or anode electrodes of pure-hydrogen and hydrogen-cesium discharges, as well as for special emitter surfaces, contacted with gas-discharge plasma, are compared. It is shown, that one of the surface-plasma channels of NI production, i.e. a low energy atom bombardment is effectively realised both in a regular surface-plasma sources, as well as in cesiated "volume" sources developed recently.

INTRODUCTION

The necessity to increase the energy of neutral beams for injection into the thermonuclear devices up to 1-1.5 MeV level requires to use the multiampere beams of Negative Ions (NI) at the acceleration stage. At present the development of the high-current stationary NI sources are carried out in two main directions.

In the surface-plasma sources (SPS) the NI production is realized on electrodes being in contact with the gas-discharge plasma. The electrodes or special emitters with a lowered work function are used in SPS for the enhancement of NI production. As a rule, the small adding of cesium into discharge are used in SPS, which allows one to obtain a manifold increase in the luminosity and intensity of the SPS produced NI beams [1-3].

In the "volume" sources NI are formed directly in plasma. An observation of the intense channel of NI production via the vibrationally excited molecules [4] makes

it possible to improve the volume sources deliberately and to go over to the elaboration of multiampere stationary models [5-7]. Recent studies have shown, that the efficiency of two-step NI production in plasma volume via the vibrationally excited molecules, which increases nonlinear with the growth of plasma and molecular hydrogen densities in the discharge, is limited at the relatively low level by the intense destruction of NI by plasma and gas.

A significant improvement of the "volume" sources characteristics has been obtained recently due to adding the small amounts of cesium into the discharge [8, 9]. As it has been shown, the processes of surface NI formation dominate in the "volume" sources with the adding of cesium or barium [10, 11], similar to those in SPS with the NI production on the anode surfaces and on the emission slit walls [12, 13]. The direct comparison of the characteristics of "pure-hydrogen" volume sources without cesium and "volume" sources with the small adding of cesium convincingly proves the high efficiency of the surface-plasma channels of NI production in hydrogen-cesium systems and additionally increases the interest to the surface NI formation processes.

A survey of the surface processes, which are relevant for NI production in the various SPS modifications and in the analogous "volume" sources with the small adding of cesium is given below. The processes of NI formation due to the impact desorption and due to the reflection of particles

are considered both for the well-defined conditions and for the case of the plasma particles interaction with the surface of electrodes, which is more typical for SPS and for cesiated "volume" sources. The efficiency of the NI production on the cathode and anode gas-discharge surfaces, as well as on the surfaces of the specially-prepared emitters, contacted with gas-discharge plasma, is discussed. The NI production efficiency in cesiated SPS is compared to that in the pure-hydrogen ones.

The investigations of the NI production on gas discharge surfaces with the use of cesium catalysis are carried out during last twenty years and were stimulated with the development of the surface-plasma methode of NI production. Most of the results have been published in the "Proceedings of the Brookhaven Symposiums on the production and neutralization of NI " [14-18]. The reviews on the surface processes of NI formation were given in [12, 19, 20].

I. NEGATIVE ION FORMATION IN THE CASE $\varphi > S$

The negative ions with a low electron affinity S can be efficiently produced on the surfaces with a work function $\varphi > S$ mainly due to the processes of non-equilibrium NI Secondary Emission. Under the non-equilibrium NISE the emitting NI overcomes the additional near-electrode barrier $\varphi - S$ due to the kinetic energy, acquired in the non-equilibrium process. The non-equilibrium pro-cesses of ions

and atoms reflection from the surface, and adsorbate or substrate sputtering (desorption) by ions, atoms, electrons, photons may lead to the NI emission under $\varphi > S$ conditions. The efficiency of the NISE processes is conveniently characterized by the NISE Coefficients R^- and Y^-, and by the Negative Ion Fraction (NIF) of the secondary particles β_r^-, β_s^-, defined by the regular portions: $R^- = I_r^-/I_i = \beta_r^- \cdot R$; $Y^- = I_r^-/I_i = \beta_s^- \cdot Y^-$, where I_i-incident flux, I_r, I_s-reflected and desorbed NI fluxes, R, Y -integral coefficients of particle reflection or desorption.

Sometimes the efficiency of NI production in gas-discharge conditions is characterized by NI yield $F^- = I^-/I_i^+$, normalized to an incident ion current I_i^+, where the NI production by neutrals is not included; or by the efficiency of "conversion" κ^- of dis-charge current I_d into an extracted NI beam $\kappa^- = I^-/I_d$.

The reflection R and desorption Y coefficients are dependent of a number of parameters as a mass, energy and an angle of incidence of bombarding particles, on substrate type and structure, on an adsorbate thickness ets. The NIF of secondary particles is determined by electronic exchange between the surface and outgoing particle. In the case $\varphi > S$ the NIF value depends on the particle outgoing velosity $v_\perp$ and is very sensitive to the surface conditions: the work function and density of electronic states n_e at the Fermi level.

NEGATIVE ION FRACTION

The direct measurements of the β^- value during the reflection of hydrogen ions from the cesium-covered surfaces of mono- and polycrystalline tungsten and from barium were carried out at FOM-Institute.

It has been experimentally proved, that at the outgoing velocities of the particle $v_\perp$, less than the velocities of electrons on the Fermi level in the metal, and at not too grazing incident angles, the NIF value is independent of the prehistory of the process, namely, of the energy, incidence angle, and the charge state of the primary particle, but is fully defined by the removal velocity $v_\perp$ and by the characteristics of the proper surface layer φ and n_e [21]. Fig.1 shows the experimental values of NIF obtained for the monocrystalline tungsten coated by the optimal cesium coverage [22] and the data for barium [23] vs the particle outgoing energy $E_\perp$. NIF has a high value (>0.5) in spite of the unfavourable relation $\varphi \simeq 2S$ for the W-Cs surface at the outgoing energy range $E_\perp \simeq$ 2-8 eV. At the optimal velocity $v_\perp = 3 \cdot 10^4$ m/s it reaches the values of $\beta^- = 0.67$.

The values of $\beta^- \simeq$ 0.3-0.2 were observed in the case of reflection from the surface with the structure W-H-Cs formed by the consecutive adsorption of hydrogen and cesium on the tungsten surface [24]. The relatively high values of $\beta^- \simeq$ 0.1-0.3 were observed for hydrogen reflection from the thick barium layer with a higher work function φ=2.5 eV and with

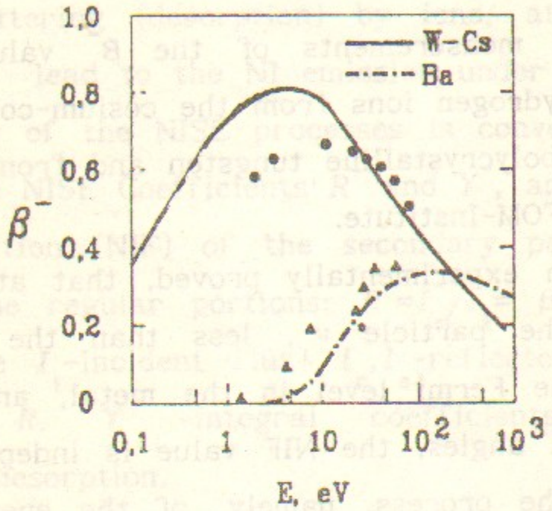

Fig. 1. Negative ion fraction of hydrogen backscattered from W–Cs and Ba surface.

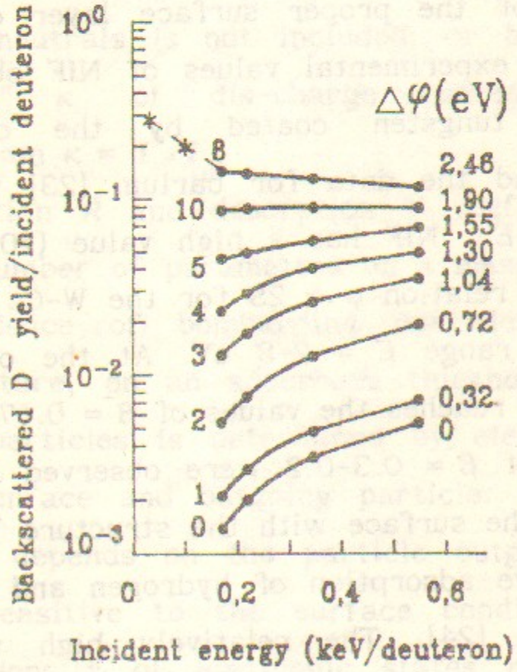

Fig. 2. Backscattered D^- yield. Cs–Ni bombarded by D_3^+ ions.

the increased, in comparison with cesium, electron density n_e [23]. The solid lines in Fig.1 show the calculated NIF values obtained with the help of probability model by the adjustment of fitting parameters.

NEGATIVE ION PRODUCTION BY BACKSATTERING

Energetic Hydrogen. Formation of NI by hydrogen and deuteron ions backscattering from alkali metal and cesiated surfaces was studied by LBL group [25]. The energy of incident particles varied in 0.15 - 4 keV range. It was found, that backscattering NI yield R^- has a larger value for the alkali metals with a larger atomic number and lower work function of the surface. During the collisions with the surface the molecular ions H_2^+, H_3^+ (D_2^+, D_3^+) dissociate and give the two or three times greater yield of $H^-(D^-)$ ions, than the ions H^+, D^+ with the corresponding equivalent energy. Fig.2 shows R^- dependences on the equivalent energy of the primary D_3^+ ions, incident normal to nickel-cesium surface [25]. The figures to the left of the curves denote the number of cesium portions, injected to nickel. The figures to the right denote the corresponding change of the Ni-Cs surface work function. For optimal cesium coverage on nickel ($\varphi \simeq 1.6$ eV) R^- reaches the value of $\simeq 0.14$ D^- per incident deuteron and is slightly diminished with an increase in the primary ions energy within 170÷550 eV/deuteron range. The extrapolation of these data to the

region of lower primary ion energies 100÷20 eV/deuteron with the use of MARLOWE code gives greater values of $R^- \simeq 0{,}2 - 0{,}26\ D^-$ per incident deuteron [26] (to points in Fig.2).

For the low cesium coverage on nickel the R^- value increases with the energy of incident particles (Fig.2). For the pure nickel surface NISEC has a value R^-=0.1% at the energy of the primary ions D_3^+ 170 eV/deuteron and increases 1.5 times due to small cesium coverage of ≃0.1 monolayer.

In the case of grazing incidence of hydrogen ions the particles reflection coefficient is greater. The values R^-=0.35 H^- per incident nucleon were detected for the hydrogen ions with an energy 400 eV/nucleon and 82° incident angle with respect to the normal to W-Cs surface (φ=1.45 eV) [29].

The cited high values of $R^- \simeq 0.2 \div 0.3$ may be realized in the reflection of fast hydrogen ions and atoms from the surfaces of cathodes, anodes or special emitters, covered with cesium and biased negatively relative to SPS plasma with the potential 100-200 V.

LOW ENERGY ATOM BOMBARDMENT

NI production by low energy hydrogen atom bombardment of cesium or cesiated surfaces was studied in several papers [27-29]. The thermal hydrogen atoms flux with the current density 10^{14}-10^{16} $cm^{-2} \cdot s^{-1}$ was created due to the dissociation of hydrogen on the surface of tungsten tube

heated up to 2500-3000 K. It has been found, that only the atoms in the tail of the Maxwellian distribution can produce NI. For a thick cesium surface ($\varphi \simeq$ 1.9 eV) the efficiency of NI production was about $K^- = R^- + Y^- \simeq 1.5 \cdot 10^{-4}$ ions per incident hydrogen atom. For the optimal sesium coverage on molybdenum (φ=1.6 eV) the efficiency of NI production was greater and increased in the range $K^- \simeq 2 \cdot 10^{-4}$-$3 \cdot 10^{-3}$ with the growth of the dissociator temperature in the interval 1700-2200 K [29]. If one takes into account only the atoms with energy greater, than 1 eV in the primary particle flux, the larger value of $\bar{K}^- \geq 0.04\ H^-$ per incident hot atom corresponded to the NI production efficiency values, obtained for Mo-Cs surface. The value $K^- = 2 \cdot 10^{-2}\ H^-$ per incident atom and recalculated value $\bar{K}^- \simeq 0.3\ H^-$ per incident atom with energy higher, than 1 eV, were obtained for cesiated silicon surfaces (φ = 1.45eV) [29].

The values $K^- \simeq$ 0.01-0.3 may be realized due to the irradi-ation of cesiated anode and "plasma" electrodes of ion sources by the fluxes of low energy atoms and ions from hydrogen plasma.

NEGATIVE ION PRODUCTION BY IMPACT DESORPTION

There are physical and chemical desorptions with different nature and efficiency exist. The physical (knockon) desorption takes place at the particle energies greater, than the threshold value, and is stipulated by the

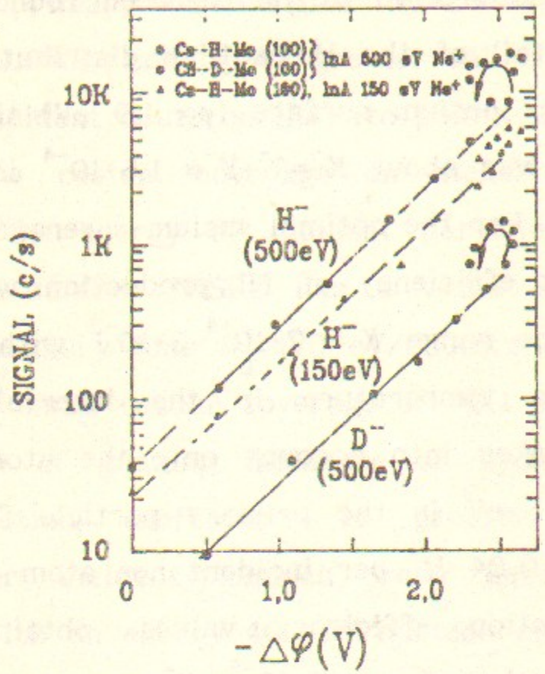

Fig. 3. H^- desorption yield as a function of $\Delta\varphi$. Incident Ne^+ beam.

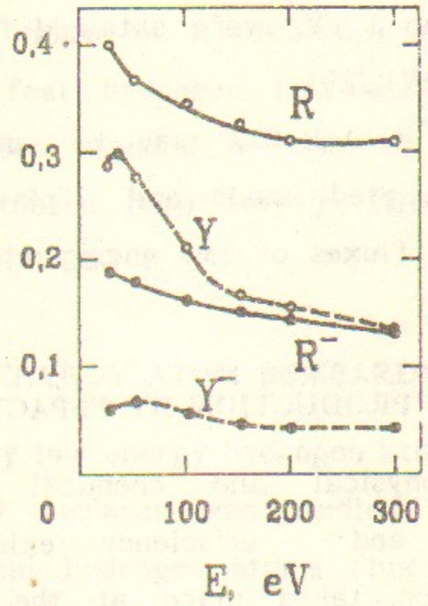

Fig. 4. The simulated coefficients R, R^-, Y, Y^- vs energy of protons. Surface MoH–Cs.

kinetic energy transfer from the incident particle to the adsorbate atoms. The chemical desorption is stipulated by the chemical reaction, caused by the incident particles. As a result of this reaction unstable or volatile compound is formed on the surface leading to the particle emission. The chemical desorption may occur up to thermal energy of incident particles and increases under the irradiation of the surface by electrons and photons. In the gas-discharge the desorption takes place mainly due to ions and atoms, while the desorption due to electrons and photons is several orders of magnitude lower [30].

Desorption by heavy particles. The measurements of the relative yield of H^- ions during the impact desorption of the Mo-H-Cs structure,created by consecutive adsorption of hydrogen and cesium on the molybdenum surface were carried out in [32]. The primary Ne^+ ions with the energies of 150 and 500 eV were incident to the surface with the angle 45°. Fig. 3 shows the variations of the desorbed H^- yield in dependence on the change $\Delta\varphi$ of the Mo-H-Cs surface work function. Initially the work function decreased due to the injection of the cesium portions, reaching its minimum $\varphi \simeq 1.6$ eV at the optimal coverage $\theta_{Cs} \simeq$ 0.6-0.7 of monolayer, and increased with further cesium injection up to the value φ = 1.9 eV corresponding to the thick cesium film. The exponential growth of yield Y^- (Fig.3) is stipulated mainly by changes of "electron" properties of the surface and

corresponding NIF changes. The "activation" loops are observed near to the optimal and at the thick cesium coverages (Fig.3). At the equal work function values NI yield was 1.5-3 times greater for higher cesium coverage. Such a behaviour is probably stipulated by an increase in the impact desorption coefficient Y itself and may be caused by the decrease in binding energy of hydrogen atoms with a surface in the case of the thick cesium coverage.

The absolute value of H^- yield, induced by the impact desorption with cesium ions was measured for Mo-H-Cs surface created by the simultaneous adsorption of hydrogen and cesium on the molybdenum [33]. With the energy of incident cesium ions $E_o \leq 200$ eV, attainable for regular SPS, the detected NISEC had a value $Y = 0.02$. For the lower cesium energy 150 eV, NISEC had a value $Y^- = 0.003$. Such a small efficiency of the hydrogen desorption by low energy cesium ions is stipulated by low energy transfer from the primary cesium ions and from knocked-on molybdenum atoms in binary collisions with hydrogen: $E_H \simeq 0.7\text{-}1.5\%\ E_o$.

For the desorption by cesium ions with an increased energy $E_o \geq 300$ eV and current density $j^+ > 10^{-4}$ A/cm^2 from Mo-H-Cs structure, created by the coadsorption of hydrogen and cesium from a gas near the surface, the detected value of Y and Y^- yields may be limited by the low rate of hydrogen and cesium delivery to the surface [34-36]. The greater Y^- values were observed at the optimal current density of the incident cesium ions [36], for hydrogen feeding through the pores in emitter [34], or in the case of the preliminary irradiation of the surface by hydrogen plasma [35]. In the last case NISEC had value of $Y^- \simeq 1.2\text{-}1.45$ at the energies of the primary cesium ions 1.-1.7 keV. This was 2-3 greater, than Y^- values observed under the optimal conditions for hydrogen and cesium coadsorption from a gas [34, 36].

The dynamically stable Mo-H-Cs coverage with the low work function $\varphi \simeq 1.6$ eV is established on the Mo-surface due to the bombardment with the low energy cesium ions (45-150 eV) [37]. Under the optimal conditions in gas-discharge SPS the share of cesium ions reaches 5-10% of the total ion current to cathode. Under the increased discharge voltage 200 V the NI desorption by cesium ($Y^- \simeq 0.02$) even for the hydrogen-enriched electrode selvage may give small contribution <2% to the desorbed from the cathode H^- flux. In the multipole SPS the contribution of the cesium desorption may be more significant with the higher potential (300-400 V) of the specially prepared convertors with respect to plasma [38].

Desorption by hydrogen particles. For the low energy of primaries $<10^2$ eV, desorption of hydrogen by light ions and atoms is more efficient, then that produced by heavy particles. The calculated cross-section of deuterium desorption from adsorbate on nickel has a value of

$1.5\text{-}1.2\cdot10^{-16}$ cm^2 [30] for the energy of hydrogen particles 50÷500 eV/nucleon, this is in a good agreement with the experiment [39]. In the particular case of stainless steel covered by deuterium ($\theta_D = 2\cdot10^{15}$ atom/cm^2) the desorption yield $Y \simeq 0.72$ atom/ion has been detected, or $\bar{Y} = 0.24$ atom/nucleon when using primary H_3^+ ions with an energy 330 eV/nucleon.

An increased energy of the particles, desorbed by light ions is favourable for their negative ionization. A computer simulation shows [40], that for the energy of incident hydrogen atoms of 300 eV, more than a half of particles, desorbed from the hydrogen on the nickel, has an energy in the 20-40 eV range.

Fig. 4 shows the computer simulations data both for the desorption yield Y and for H^- yield Y^- [41]. The impinging protons were incident normal to the surface of the amorphous molybdenum, saturated with interstitial hydrogen and covered by optimal cesium film. The stoichiometric formula of the target was Mo_1H_1, the corresponding surface hydrogen coverage $7\cdot10^{14}$ atoms/cm^2. The H^- yield Y^-, calculated for the desorption is slightly changed with an increase of protons energy in the range 25-300 eV and has a value $Y^- \simeq$ 6-8% (Fig.4).

Fig.4 also shows the calculated values of the reflection coefficients R and R^- for the reflection of hydrogen from MoH-Cs structure. In the tested range of proton energy

calculated R^- values are ≃3 times greater, than the corresponding values Y^- for the desorption by protons.

NISE efficiencies data are listed below for various SPS particles with normal incidence to the cesiated molybdenum surface are listed in table.

Table

NISE Efficiency Data for Variuos SPS Particles with Normal Incidence to Cesiated Molybdenum

Energy, eV	Particle	Process	$K^-=I^-/I_i$, %
10 - 100	H^0	Reflection	26 - 22
		Desorption	6 - 8
	H^+	R	22 - 18
		D	7 - 6
100 - 150	H_2^+	R	50 - 45
		D	16 - 14
	H_3^+	R	75 - 70
		D	20 - 24
150 - 200	Cs^+	D	0,3 - 2
1 - 3	H^0	$R + D$	4 - 30

Electron- and photon-stimulated desorption. Electrons and photons may excite the electronic states of the adsorbed particles, providing their connection with the remaining

ensemble, and transfer them to the repulsing states. The features of electron-stimulated desorption (ESD) are discussed in review [31]. These comparative investigations of ESD of H^-, D^- ions and their emission during the bombardment by cesium ions were carried out in [42]. The studies of ESD were conducted during the coadsorption of residual gas molecules ($p \simeq 2\text{-}3\cdot10^{-4}$ Pa) and potassium on the moly. ESD of H^- ions became manifold stronger for the optimal potassium coverage on the moly. The mass-spectrum of electron-desorbed and cesium-desorbed NI differs significantly. Mainly the negative ions of hydrogen and deuterium are emitted due to ESD, whereas the impurities of O^-, OH^-, C^- etc. are preferably desorbed during the ion bombardment [42].

Under the "pure" conditions the efficiency of ESD of atoms reaches the values $Y^-=5\cdot10^{-7}$ atom/electron, whereas the effici-ency of emission of ions $Y^{\pm} \simeq 10^{-2}$ Y [31]. The H^- yield with intensity of 10 A was obtained by laser irradiation of NaH target with CO_2-laser pulse energy 6J and pulse duration 200 ns [43].

II. NEGATIVE ION PRODUCTION ON SURFACES IN THE PLASMA ENVIRONMENT

The efficiency of NI formation in single events of bombardment may be high, but it cannot guarantee an efficient production of intense H^- fluxes. Fortunately, an

intense NI production with an average conversion $\kappa^-=I^-/I_d^- \simeq$ 0,12-0.17 was obtained in several modifications of SPS under "dirty" gas-discharge conditions and an intense bombardment of the electrodes [12, 13].

The "efficient" NI yield per incident positive ion had rather high value F^-=0,8 [12]. It clearly demonstrates that NI production efficiency may be higher under gas-discharge conditions than in separate processes under well-defined conditions.

Activation of Surface NI Production by Plasma. The effects of plasma on surface NI production enhancement were observed. An additional reduction of the electrode work function caused by plasma activation of electrode it was found. Activated by hydrogen-cesium discharge Cu-electrode had the work function $\varphi\simeq$1,38 eV [44]. This value was lower, than that reported for optimum coverage of Cs on Cu.

The fueling of the electrode selvage with a plasma increased the efficiency of H^- desorption 2-3 times compared to maximum values, obtained with other ways of fueling [34,35]. Both effects of the work function lowering and of the desorption yield increase by plasma fueling can enhance the NI production in SPS.

Synergetics. The 10-fold enhancement of NI production during the simultaneous hydrogen and heavy ion bombardment of cesiated electrodes was found by Seidl et al [45] and by van Os et al [46].I n the absence (or at low level) of heavy

ion bombardment the efficiency of H^- production caused by the only hydrogen ion bombardment had the substentially lower value. On the other hand, the only heavy ion bombardment had low efficiency, so the simultaneous bombardment produced H^- yield higher, than the sum of the individual processes. It seems that an optimal (5-10% of total incident current) heavy component is necessary for removing of an excess in cesium coverage of surface and for activation of the surface by sputtering some contaminations (oxides, carbides) from cesiated electrodes.

The resulting NI Yield $K^- = Y^- + R^-$ per incident ion with the energy of 200 eV had the higher value $K^- = 0{,}31$ under optimized synergetic bombardment conditions [45]. This value was similar to the peak value of $K^- \simeq 0{,}37$, measured during bombardment of cesiated molybdenum by hydrogen ions from gas-discharge plasma [47].

III. EFFICIENCY OF NI PRODUCTION IN SPS

A number of SPS modifications are developed for accelerator and fusion injector usage. Pulsed multiaperture honeycomb SPS produces the H^- beams with the intensity of up to 11 A and pulse gas efficiency ≃20% [48]. H^- current density in the emission holes of SPS exceeds 8 A/cm^2 [49]. SPS with modified PIG geometry delivers the H^- beams with the highest luminosity $\simeq 10^8$ A/cm^2 rad^2 [50]. The "conversion" of discharge current into SPS produced H^- beams had the value $\kappa^- \simeq 17\%$ for grooved semiplanotron SPS [13].

High parameters of SPS are provided by the effective surface processes of NI production in plasma environment and by plasma ensured an intense electrode bombardment, "self-extraction" and transport of surface-produced NI [12]. Several elementary processes involved in NI production on the cathode, anode and special emitter surface of SPS. Relative contribution of individual processes and efficiency of NI production depends on the SPS geometry and discharge mode. Schematic view of several SPS modifications with specific surface-plasma channels of NI production are shown in Fig.5.

SPS WITH GEOMETRICAL FOCUSING

In the advanced SPS with geometrical focusing (GF) of NI the H^- yield are increased by concaving the emitting surface of cathode and by focusing of the emitted NI with a concaved near-electrode electric field. SPS with one-dimensional GF utilize grooved cathodes and longitudinal emission slits [51, 52]. SPS with two-dimensional GF use spherical cathode concavities and round emission holes [57, 58]. The desorbed and low energy reflected NI fractions are focused better during the post-acceleration with near-electrode electric field due to it lower energy and angular spread. It was clearly demonstrated by measurements of energy and angular

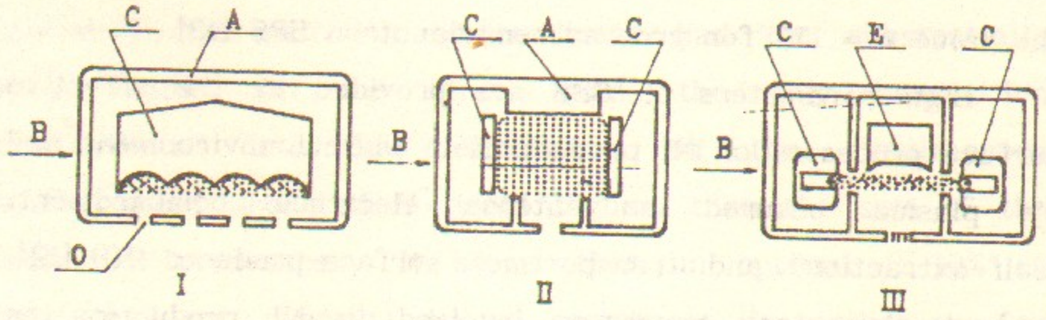

Fig. 5. Schematic view of several SPS. I – semiplanotron, II – PIG, III – hollow cathode PIG with independent emitter; A – anode, C – cathode, E – emitter, B – magnetic field, O – emission orifice.

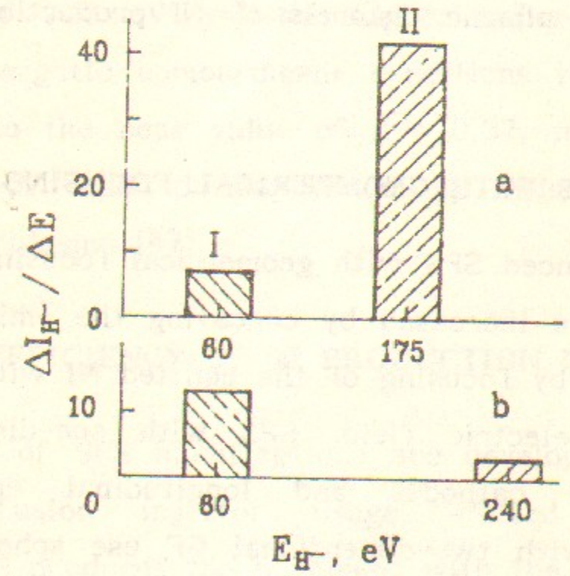

Fig. 6. The energy composition of H^- from honeycomb SPS : a – emission hole at GF point; b – emission hole far from GF point.

spread of surface produced NI [53] and by measured composition of NI beam extracted at various positions of emission hole relative to GF point [54].

There are there main groups of NI extracted from a honeycomb SPS (Fig.6). The first H^- group had an average energy ≈60 eV relative to anode potential and was generated mainly due to fast hydrogen atom reflection from the cesiated emission hole walls. The second H^- group with an average energy ≈175 eV was generated due to **desorption** from the cathode. With the standard position of emis-sion hole at GF point about 80% of H^- extracted were produced due to desorption from the cathode (at the temperate level of SPS discharge current). The third H^- group with an average energy 240 eV was generated due to reflection from the cathode.

The average conversion of discharge current into cathode desorbed H^- ion yield for pulse mode of honeycomb SPS was κ_d^-= 2% The measurements of cathode current composition indicates that at discharge current density ≈10 A/cm^2 approximately 30% of current to the cathode consists of positive ions and relations between the positive components are: $I_{H^+} : I_{H_2^+} : I_{H_3^+} : I_{Cs^+}$=3:3:3:1.

Taking into account the permeability μ of cathode produced NI flux through the emission hole and plasma layer (μ=0,3 in this particular case [41, 54]) it is possible to evaluate the effective **desorption** yield, normalized to

number of nucleons in incident positive hydrogen ion flux: $\bar{Y}^- \simeq 0{,}1\ H^-$ per incident nucleon.

This rather high value of the "effective" desorption yield on cathodes of SPS must be corrected by including into the incident flux a number of fast hydrogen atoms, reflected from the opposite parts of gas-discharge chamber and returned to cathode with typical for anode reflected H^- group energy (Fig.6). An average hydrogen nucleon reflection coefficient from molybdenum cathode has value $R_N \simeq 0{,}4\text{-}0{,}6$. After the second reflection from the anode approximately R_N^2 part of fast hydrogen nucleons returns to cathode and increases an incident nucleon flux 15-35% of charged particle flux. So, an efficient **desorption yield**, normalized to incident fast hydrogen nucleon flux for cesiated molybdenum cathodes of SPS has the value $Y^- \simeq 0{,}07 \div 0{,}08\ H^-$ per incident hydrogen nucleon.

H^- ions produced by desorption with Cs^+ ions have the lower energy spread and better permeability through the emission hole. But relatively small amount of Cs^+ ions compared to a number of hydrogen nucleons and lower value of hydrogen desorption by cesium seems produced negligible direct contribution of Cs^+ ions into observed canthode desorption yield (in this particular case).

The efficiency of NI formation due to **reflection** of fast hydrogen particles from cesiated SPS cathodes can be estimated by comparison of the concave cathode "desorption"

data with the H^- emission from flat cathodes. In the case of a large flat cathode surface and small emission slit with thin walls the transmission of reflected and desorbed NI fractions had the same value. The conversion of discharge current density into the cathode produced H^- current density for flat cathode had the maximum value $\kappa^- \simeq 0{,}17$. The difference between this κ^- value and the corrected "initial" desorbed fraction contribution $\bar{\kappa}_d^- = \kappa_d^-/\mu = 0{,}06$ will present a contribution of reflection $\kappa_R^- \simeq 0{,}1$ into the cathode NI production. At the listed earlier relative value and composition of positive ion current to the cathode it gives for the normalized **reflection yield** from SPS cathode the value $R^- \simeq 0{,}13\text{-}0{,}15\ H^-$ per incident hydrogen nucleon. The total efficiency of NI production due to reflection exceeds the desorption NI yield under SPS discharge conditions.

An efficiency of the cathode and anode NI production and its relative contribution into the SPS H^- output can be found from the dependencies of extracted NI yield on discharge current. A number of such dependencies [50] are shown in Fig.7 for the groove semiplanotron SPS with different emission slit geometries (curves 1-6) and for PIG version of SPS (curve 7).

The sharp initial growth of H^- beam current in discharge current range 0-30 A of Fig.7 caused mainly due to an increase of cathode NI production processes. With an increase of the discharge current and plasma density the

cathode produced H^- ions strongly attenuated in collisions with plasma particles during its motion to emission orifice. Further increase in H^- current in the discharge current range 60-120 A (Fig.7) was mainly caused by NI formation on emission slit anode walls. The slope of anode section of the curves indicates that the anode NI production had the same efficiency for various profiles of the thick emission slits (curves 1-4, 6) and doubled with a decrease in the emission slit thickness (curves 5, 7). Under the optimal conditions (h= 1 mm, θ=60°) an anode conversion efficiency with the value $\Delta I^-/\Delta I_D \simeq$ 0,5% was regularly revealed for the multigroove [13] and honeycomb SPS [49]. At the high discharge current of these SPS approximately one half of the extracted H^- beam was the anode produced one.

The main processes involved into anode H^- production are the reflection and desorption by fast group of hydrogen atoms, originated due to reflection of positive ions from cathode, and the reflection (desorption) of low energy hydrogen atoms, produced in plasma or due to desorption from electrodes. Fast hydrogen atoms with a flux density up to 2,7 A/cm^2 was measured at SPS discharge current density 10 A/cm^2 [55]. The intense flux (≃ 5-30 A/cm^2) of low energy hydrogen atoms (T_H= 1-2 eV) must irradiate the anode surfaces, as it indicates by spectroscopic measurements of SPS hydrogen density and temperature [56, 57]. An average energy of the anode produced NI, extracted from SPS with GF,

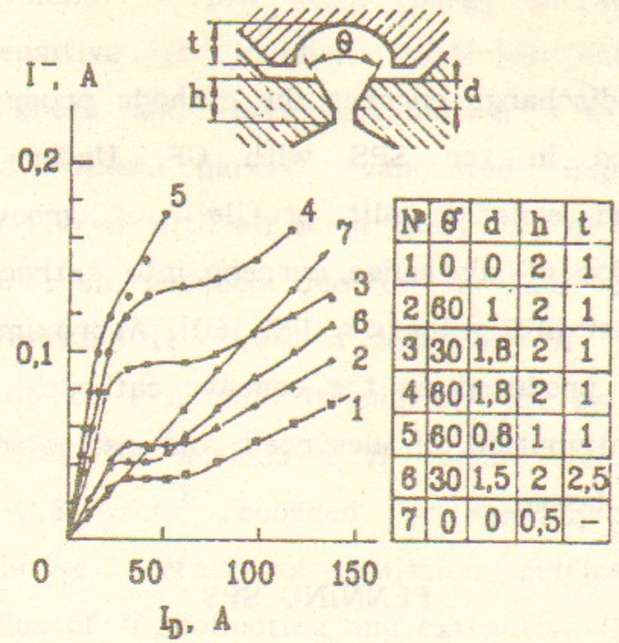

№	θ°	d	h	t
1	0	0	2	1
2	60	1	2	1
3	30	1,8	2	1
4	60	1,8	2	1
5	60	0,8	1	1
6	30	1,5	2	2,5
7	0	0	0,5	–

Fig. 7. H^- current I^- vs discharge current I_D for different geometries of emission slit. 7 – curve for PIG geometry.

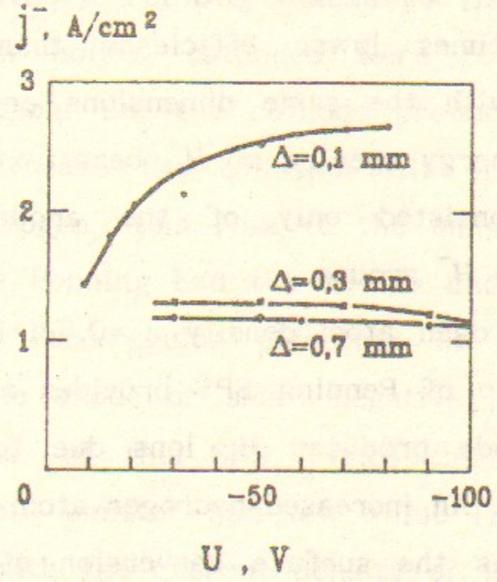

Fig. 8. H^- current density j^- vs voltage on emitter U_e for different distance Δ between emitter and plasma layer.

corresponds to reflected fraction of incident fast hydrogen atoms (Fig.6).

At low discharge current the cathode produced NI group are dominated in the SPS with GF. Under the optimal conditions and emission slit profile of grooved SPS the total conversion of discharge current into extracted H^- beam had the highest SPS value $\kappa^- \simeq$ 17% [60]. Approximately 80% of H^- beam was produced on the concave cathode surface with the same contribution of desorbed and reflected group into the extracted beam.

PENNING SPS

In Penning SPS cathode produced H^- ions can not directly reach the anode emission orifice outlet. As a result, the conversion of Penning gas-discharge current into H^- beam had at least two times lower efficiency than that for the planotron SPS with the same dimensions and under optimal conditions. An energy spectra of H^- beam extracted from the Penning SPS consisted only of the anode produced and charge-exchanged H^- groups.

A high hydrogen atom density n_H=0.5-1$\circ 10^{15}$ cm^{-3} in the near anode region of Penning SPS provides an effective conversion of cathode produced H^- ions due to volume charge exchange process. An increased hydrogen atom temperature T_H = 1-2 eV facilitates the surface conversion of hydrogen atom flux to NI on the cesiated SPS electrodes.

The efficiency of low atom energy surface conversion are very sensitive to incident particles energy, cesium coverage thickness and its contamination with the oxides, carbides and other hardly evaporated impurities. The incident atom fluxes with an atom energy ≥1 eV and intensity of ≃30 A/cm^2 can produce due to sur-face conversion on cesiated molybdenum (K^-=0,04) a secondary H^- flux with an intensity of up to 1 A/cm^2. It can provide an appre-ciable contribution into the measured H^- beam emission current density of 2-2,8 A/cm^2, recorded for Penning SPS with an increased relative surface of emission orifice walls and optimized angles of H^- collecting and extraction (Fig.7).

An effective anode surface production of H^- ions with the emission current density of up to 2 A/cm^2 was observed in the **hollow cathode Penning discharge** [12, p.93]. In this case (Fig.5) both hollow cathodes were too distant from emission slits region. So, the cathode produced NI and fast atoms could not reach the emission slit area at all. The residual fast hydrogen atom flux to the emission slits walls of hollow cathode Penning had the energy and intensity much lower, than that for regular planotron or PIG SPS modi-fications. With the anode or small negative potential on the independent emitter of this SPS (Fig.5) the incident positi-ve ion current into emitter had low value [12] and the ob-served H^- yield with the current density of up to 1,5 A/cm^2 (see Fig.8) was caused mainly by the production on emission

slits walls. In the experiments with a small emission slit (0,37×2,25 mm) the anode wall production with intensity of extracted H^- beam up to 2-2,7 A/cm ^{2}was recorded [12].

Recent experiments with the hollow cathode Penning discharge showed, that the anode production mechanism provides easily an intense quasi-stationary beams of H^- ions with current density in the emission holes of up to 1 A/cm^2 and an average H^- beam current density of 0,1 A/cm^2 in large multiaperture extraction area [58].

SPS WITH SPECIAL EMITTERS (CONVERTORS)

The NI production and yield are remarkably increasing with the special "independent" emitter (convertor) biasing negatively to plasma potential (Fig.8). An overall conversion efficiency of the emitter current I_e into a NI yield I^- had the value $\kappa_e^- = \Delta I^-/I_e \simeq$ 2,5-5,5% under the optimal potential of the emitter $U_e \simeq$ 130-210 V for several SPS modifications [59-62]. Relatively low value of κ_e^- compared to value $\kappa^- \simeq$ 17% observed for "cathode" region of dependencies (Fig.7) [13, 58] is probably caused by the lower transparency of exit apertures in the experiments [59,62] for the hydrogen-desorbed and reflected groups of H^- ions and by larger contribution of secondary electrons into the collec-tor current recorded. As a result, the cesium-desorbed fraction of H^- flux dominate in the energy

spectra of H^- beam [63]. The contamination of an independent emitter (convertor) lower the H^- ion production efficiency significantly [64].

PURE-HYDROGEN SPS

There are several attempts were undertaken for eliminating even small amounts of cesium from SPS operation. An appreciable yield of H^- ions was recorded for Pure-Hydrogen Discharges (PHD) with the electrodes, made of pure molybdenum [2, 65] or with the LaB_6 cathodes [66].

The energy spectra of H^- ions extracted from PHD of semiplanotron SPS [54] are shown in Fig.9. About 25% of the extracted NI were produced due to reflection of hydrogen particles from molybdenum cathode and had an energy in the range 1,1-1,9 (eU_d+eU_0), where U_d-discharge voltage, U_0-extraction voltage, applied to external anode of gas discharge chamber. The main part of extracted NI with an energy 0,4-0,8$\cdot(eU_d+eU_o)$ was produced due to reflection from emission hole walls. The surface produced NI dominated over the volume0 produced NI (group I in Fig.9) under the optimal conditions of PHD of semiplanotron.

The energy spectra and value of H^- yield, as well as measured composition of PHD discharge current onto the cathode,shows that the efficient NISEC for reflection on the cathode has had the value R^-=0,5-0,7% H^- per incident hydrogen nucleon. This value does not contradict the value

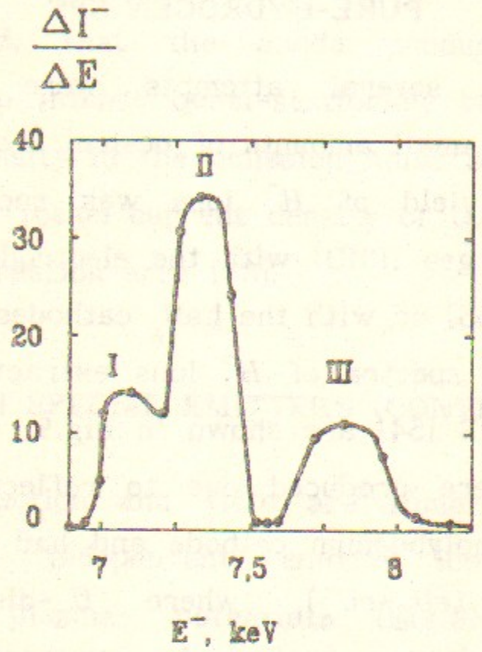

Fig. 9. Energy spectra of H^- extracted from Pure-hydrogen SPS with extraction voltage 7 kV. Discharge voltage 550 ± 50 V.

measured for pure or weakly activated nickel under the well-defined conditions (Fig.2).

More intense anode surface production (Fig.9) is caused due to larger grazing incidence reflection of fast hydrogen atoms and due to the increased "effective" area of emission hole cones surface.

As a whole, the PHD semiplanotron delivers the H^- beams with an emission current density of up to 1,1 A/cm^2. An H^- beams with current up to 1 A were obtained with a multislit extraction from PHD semiplanotron [65].

REFERENCES

1. *Yu.Belchenko, G.Dimov, V.Dudnikov.* Doklady AN SSSR, **213**, 1283 (1973) (Reports of USSR Academy of Sciences - in Russian).
2. *Yu.Belchenko, G.Dimov, V.Dudnikov.* Nuclear fusion, **14**, 113 (1974).
3. *K.W.Ehlers and K.N.Leung.* Rev. Sci. Instrum, **51**, 721 (1980).
4. *M.Allan and S.Wong.* Phys. Rev. Lett., **41**, 1791 (1978).
5. *M.Bacal, E.Nicolopoulou and H.Douset.* p.26 in Ref. 14.
6. *K.N.Leung, K.W.Ehlers, R.V.Pyle.* Rev. Sci. Instrum., **56**, 364 (1985).
7. *M.Hanada, T.Inoue et al.* Rev. Sci. Instrum., **61**, N 1 (2), (1990).

8. *S.R.Waltner, K.N.Leung, W.B. Kunkel.* J. Appl. Phys., 64, 3424 (1988).
9. *Y.Okumura, M.Hahada, T.Inoue et al.* p.169 in Ref.18.
10. *K.N.Leung, S.Waltner, W.B.Kunkel.* Phys. Rev. Lett., 62, 764 (1989).
11. *Y.Mori, T.Okuyama, A.Takagi and D.Yuan.* KEK Preprint. Nucl. Instrum and Meth. **A301**, 1 (1991).
12. *Yu.Belchenko, G.Dimov, V.Dudnikov.* p.79 in Ref. 14.
13. *Yu.Belchenko, V.Dudnikov.* Proc. of XV Int. Conf. on Phenomena in Ion. Gases, Minsk, 1981, part II, p-1504.
14. Proceedings of the International Symp. On the production and neutralization of negative hydrogen ions and beams /Ed. by Kh. Prelec.- N.Y.: BNL-50727, 1977.
15. Proceedings of the second International Symposium on the production and neutralization of negative hydrogen ions and beams /Ed. by Th.Sluyters.-N.Y.:BNL-51304, 1980.
16. Production and neutralization of negative ions and beams (3rd International symp., Brookhaven 1983) /Ed. Kr. Prelec.: AIP Conf. Proc. No 111.-N.Y.:1984.
17. Production and neutralization of negative ions and beams (4th International symp., Brookhaven 1986) /Ed. J.Alessi.: AIP Conf. Proc. No 158.-N.Y.: 1987.
18. Production and neutralization of negative ions and beams (5th Internat. symp., Brookhaven 1989) / Ed. A.Hershcovitch: AIP Conf. Proc. No 210.-N.Y.: 1990.
19. *J. Hiskes.* J. Phys. (Paris), **40**, c7-179 (1979).

20. *A.Kleyn.* p.3 in Ref. 18.
21. *J.van Wunnik, B.Rasser and J.Los.* Phys. Lett., **87A**, 288 (1982).
22. *J.J.C.Geerlings, P.W. van Amersfoort, L.F.T. Kwakman et al.* Surf. Sci., 157, 151 (1985).
23. *C. van Os, P. van Amersfoort, J.Los.* J.Appl. Phys., 64, 3863 (1988).
24. *P.W. van Amersfoort, J.J. Geerlings, R. Rodink et al.* J. Appl. Phys., 59, 241 (1986).
25. *P.J.Schneider, K.H.Berkner, W.G.Graham et al.* Phys. Rev., **23B**, 941 (1981)
26. *J.R.Hiskes and P.J.Schneider.* J. Nucl. Mat., **93-94**, 536 (1980).
27. *W.G.Graham.* Phys. Lett., **73A**, 186 (1979).
28. *A.Pargelis and M.Seidl.* Phys. Rev., **25B**, 4356 (1982).
29. *M.Seidl, W.E.Carr, J.L.Lopes and S.T.Melnichuk.* "Proc.III Eur. Workshop on Prod. and Appl. of NI, Amersfoort, 1988 ". Edited by H.Hopman and P.van Amersvoort, FOM-Inst., Amsterdam, p.157.
30. *E.Taglaver.* Nuclear Fusion. Special issue;"Data compendium for plasma-surface interaction", p.117, (1984).
31. *V.N.Ageev, O.V.Burmistrova, Yu.A. Kuznetsov.* Uspekhi Fiziche - skikh Nauk, **158**, 389 (1989) - in Russian.
32. *M.Yu.* p.48 in Ref. 14.
33. *J.L.Lopes, J.A.Greer and M.Seidl.* J. Appl. Phys., 60, 17 (1986).

34. *E.D.Bender, G.I.Dimov, M.Kishinevskiy.* Preprint IYaF N 75-9, Novosibirsk, 1975 -in Russian.

35. *E.D. Bender, M. Kishinevskiy, I.I. Morozov.* p.60 in Ref. 14.

36. *J.A.Greer and M.Seidl.* p.223 in Ref. 16.

37. *G.S.Tompa, W.E.Carr, M.Seidl.* Appl. Phys. Lett., **48**, 1048 (1986).

38. *P.van Bommel, K.N.Leung, K.W.Ehlers.* J.Appl, Phys., **56**, 751 (1984).

39. *R.Bastasz and L.G.Haggmark.* J. Nucl. Mat., **111-112**, 805 (1982).

40. *E.Taglaver and U.Beitat.* Jour. Nucl. Mat., **111-112**, 800 (1982).

41. *Yu.I.Belchenko and A.S.Kupriyanov.* Revue Phys.Appl., (Paris), **23**, 1895 (1988).

42. *A.Ayukhanov, E.Turmashev.* Zh.T.F., **47**, 2216 (1977) (in Russian).

43. *A.Y.Wong, J.M.Dawson, W.Gekelman and Z.Lucky.* Appl. Phys. Lett., **25**, 579 (1974).

44. *M.Wada, K.H.Berkner, R.V.Pyle and J.W.Stearns.* J. Vac. Sci. Technol., **A 1** (2), 981 (1983).

45. *M.Seidl, W.E.Carr, J.L.Lopes et al.* p.437 in Ref. 17.

46. *C. van Os and P.van Amersfoort.* Appl. Phys. Lett., **50**, 662 (1987).

47. *H.-M.Katsch and K. Wiesemann.* p.256 in Ref. 16.

48. *Yu.I.Belchenko and G.I.Dimov.* p.363 in Ref. 16.

49. *Yu.I.Belchenko.* Fizika Plazmy, 9, 1219 (1983).

50. *G.E.Derevyankin and V.G.Dudnikov.* p.395 in Ref. 17.

51. *Yu.I.Belchenko and V.G.Dudnikov.* J. de Phys. (Paris), **40**, Colloque C7, No.7, p.C7-501 (1979).

52. *J.G.Alessi and Th.Sluyters.* Rev. Sci.Instrum., **51**, 1630 (1980).

53. *M.Wada, R.V.Pyle and J.W.Slearns.* p.247 in Ref. 16.

54. *Yu.I.Belchenko and A.S.Kupriyanov.* p.198 in Ref. 18.

55. *V.G.Dudnikov and G.I.Fiksel.* Fizika Plazmy, **7**, 283 (1981).

56. *H.V.Smith Jr, P.Allison, E.J.Pitcher et el.* p.462 in Ref. 18

57. *V.V.Antsiferov, V.V.Beskorovayniy et al.* p.427 in Ref. 18.

58. *Yu.I.Belchenko and A.S.Kupriyanov.* to be published.

59. *A.I.Hershcovitch, V.J.Kovarik and K.Prelec.* Rev. Sci. Instrum., **57**, 827, (1986).

60. *K.N.Leung and K.W.Ehlers.* Rev. Sci. Instrum., **53**, 803 (1982).

61. *J.W.Kwan, G.D.Ackerman, O.A.Anderson et al.* Rev. Sci. Instrum., **57**, 831, (1986).

62. *B.Piosczyk and G.Dammertz.* Rev.Sci.Instrum., p.**57**, 840 (1986).

63. *K.N.Leung and K.W.Ehlers.* J.Vac. Sci. Technol., **A3**, 1240 (1985).

64. *C.F.A. van Os, K.N.Leung, A.F.Lietzke et al.* .17 in Ref.18.

65. *Yu.I.Belchenko, A.S.Kupriyanov,* Revue Phys. Appl., 23, 1889 (1988).

66. *K.N.Leung, G.J.de Vries, K.W.Ehlers et al.* p.356 in Ref 17.

Yu. I. Belchenko

Surface Negative Iov Production in Ion Sources

Ю.И. Бельченко

Процессы образования отрицательных ионов на поверхностях источников ионов

Ответственный за выпуск С.Г. Попов

Работа поступила 3 апреля 1991 г.
Подписано в печать 3 апреля 1991 г.
Формат бумаги 60X90 1/16.
Объем 1,7 печ.л., 1,4 уч-изд.л.
Тираж 200 экз. Бесплатно. Заказ N 27.

Ротапринт ИЯФ СО АН СССР,
г. Новосибирск, 90.